SYNTHESIS AND LUMINESCENT PROPERTIES OF Eu^{3+} ACTIVATED CALCIUM SILICATE NANOPHOSPHOR

[1]Sathish. K. N, [2]Chikkahanumantharayappa, [3],*B. M. Manohara, [4]B.M. Nagabhushana,

[1]Department of Physic, Government First Grade College, Chickballapur-562101, India.

[2]Department of Physics, Vivekananda Degree College, Bengaluru-560055, India.

[3]Department of Physics, Government First Grade College, Davangere-577004, India.

[4]Department of Chemistry, M.S. Ramaiah Institute of Technology, Bengaluru-560054, India,

Abstract : (1-9 mol %) Eu^{3+} doped CaSiO$_3$ nanophosphors have been prepared by a solution combustion technique. The phosphors have been well characterized by powder X-ray diffraction (*PXRD*), Field emission scanning electron microscopy (FESEM), Fourier transform infrared spectroscopy (FTIR) and UV Visible spectroscopy. PXRD patterns reveal monoclinic CaSiO$_3$ phase which can be obtained for calcining the samples at 900 °C for 3 h and the average particle size of the prepared samples is in the range of (30-40) nm as calculated by Scherer's formula and well mached with W-H plots. The FESEM micrographs show that crystallites are of agglomerated and irregular shape. Fourier infrared *(FTIR)* spectroscopic analysis confirms the purity of the samples. The energy band gap of all prepared samples are in the range of (4.0-4.2) eV obtain by diffused reflectance spectra (DRS). Photoluminescence spectra (*PL*) of the phosphors recorded for excitation wavelength at 316 nm show characteristic emission 615 nm of transition $^5D_0 \rightarrow ^7F_9$ of the Eu^{3+} ions. Since CIE and CCT values are situated in the red regions, prepared phosphor might be useful in red component of WLED's and can also be used in solid state display applications.

IndexTerms **- Solution Combustion, Excitation spectra, WLED, Display applications,**

I. INTRODUCTION

The study of nanomaterials have fascinated many researchers due to its unique physical, chemical, electrical and optical properties when compared to the bulk counterparts [1]. The development of low cost, highly stable, with high yield nanophosphors is in demand for display applications. In this regard, a group of researchers is concentrating on the study of cheaply and abundantly available silicate nanomaterials in the field the luminescence. A silicate host material has multi-color phosphorescence, resistance to acid, alkali and oxygen [2]. When silicate doped with active rare earth ions they become phosphor materials which has a potential applications in the field of luminescence, displays, lasers, scintillators, in safety indicators, emergency lighting such as road signs [3-4]. Various silicate hosts have been well studied by doping with rare earth and transition metal ions namely Ba$_2$SiO$_4$:Eu^{2+}, Sr$_2$SiO$_4$:Pr^{3+}, Mg$_2$SiO$_4$:Tb^{3+}, Zn$_2$SiO$_4$:Mn^{2+}, Mg$_2$SiO$_4$:Eu^{3+}, Mg$_2$SiO$_4$:Dy^{3+}, Mn, Sr$_2$SiO$_4$:Pr^{3+} [4-14]. Among these CaSiO$_3$ host exhibits a remarkable optical and luminescent properties. It exhibits ionic and covalent nature due to the presence of Ca^{2+} ions and strong interaction between Si-O, present in the SiO$_3$ group. The crystal structure of CaSiO$_3$ is having one dimensional chain of edge-sharing SiO$_4$ tetrahedron as a result transition metal ions can be easily implanted into the host by replacing the Ca site. However for rare earth ions dopant in order to maintain charge neutrality the charge compensation of Ca^{2+} and O^{2-} were considered. These dopants act as an impurity ion which results in the creation of traps at appropriate depths which stores the excitation energy and emit the light in the visible range [15, 16]. However, they show huge potential for practical applications in the field of thermo and photoluminescence.

Photoluminescence (PL) studies mainly depend on particle size, type of dopant, morphology, crystallization, growth mechanism, local symmetry, host matrix, synthesis methods. Therefore, to improve the structural properties of the luminescent materials the exothermic reaction based solution combustion technique [17] which serves as a fast and efficient method is used for the preparation of the CaSiO$_3$:Eu^{3+} nanophosphor materials. In the present work, we report for the first time the synthesis of CaSiO$_3$:Eu^{3+} (1-9 mol%) nanophosphors using citric acid as a fuel and fumed silica (SiO$_2$) as silica source by solution combustion technique. The nanopowders were well characterized by powder X-ray diffraction (PXRD), Field Emission Scanning electron microscope (FESEM). The structural and photoluminescent properties were studied and results are discussed in detail.

II. PREPARATION OF (1-9 mol %) CaSiO$_3$:Eu^{3+} NANOPHOSPHORS

CaSiO$_3$:Eu^{3+} (1-9 mol %) nanophosphors were synthesized by solution combustion method by using Citric acid as a fuel and fumed silica (SiO$_2$) as silica source [18]. The stiochiometric composition of the redox mixture was calculated by taking the ratio of total oxidizing valencies (O) to the reducing valencies (F) equal to unity i.e., (O/F=1) so that maximum energy is released during combustion. The procedure for the preparation of (1-9 mol%) Eu^{3+} doped CaSiO$_3$ nanophosphor. is shown in flow chart of Fig.1. The chemicals used for the preparation were of analytical grade and are not purified further. Calcium nitrate (Ca(NO$_3$)$_2$·4H$_2$O; sigma aldrich, 99.9 %), silica fumes (SiO$_2$, 99.9 %, surface area 200 m^2/g), Europium nitrate (Eu(NO$_3$)$_3$·5H$_2$O 99.9 %) and Citric acid (C$_6$H$_8$O$_7$) were used as the starting materials. An appropriate amount of Ca(NO$_3$)$_2$·4H$_2$O, SiO$_2$ and C$_6$H$_8$O$_7$ (1:1:1.25 in mole ratio) are well dissolved in a ~200 ml of double distilled water. The homogenized aqueous solution was obtained by magnetic stirring and adding by (1-9 mol %) europium nitrate. In the next step, the heterogeneous mixture was rapidly heated in a preheated muffle furnace at 500± 10 °C. The reaction takes place within few seconds by heating the redox mixture to incandescence leading to the formation of voluminous foamy white powder. The obtained final product was further calcined at 900 °C for 3 h for the formation of crystalline nature and used for characterization and Photoluminescence studies.
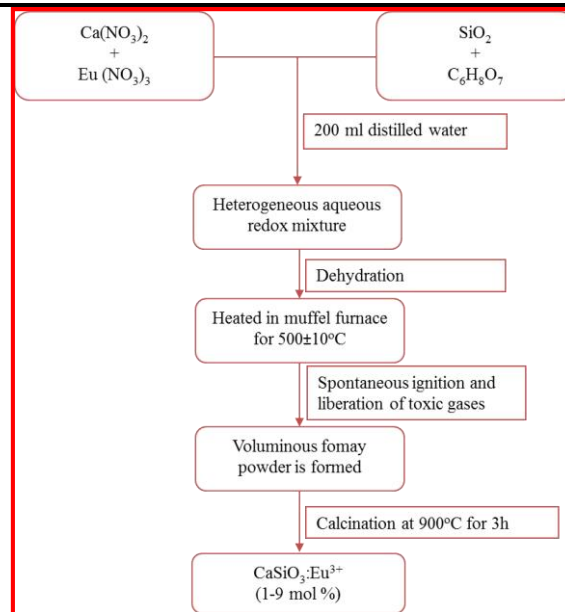
Fig.1. Flow chart for the preparation of (1-9 mol %) $CaSiO_3$:Eu^{3+} nanophosphor by solution combustion technique.

The powder X-ray diffraction (PXRD) patters were recorded on X'PERT pro Philips analytical diffractometer using CuK_α radiation (λ=1.54 nm). Morphology of the sample was analyzed by using a field emission scanning electron microscope (FESEM) (ULTRA55, FESEM (Carl Zeiss) with EDS. An FTIR study of the sample was performed with a Perkin Elmer FTIR spectrophotometer (Spectrum-1000). The UV Visible optical absorption study of the sample was made in the range 200–800 nm using Perkin Elmer Lambda 19 to obtain diffused reflectance spectra (DRS). Photoluminescent measurements were carried out using Agilent technologies, model Cary Eclipse, Spectrofluoremeter.

III. RESULTS AND DISCUSSION

Fig. 2 shows the Powder X-ray diffraction pattern (PXRD) of (1-9 mol %) $CaSiO_3$:Eu^{3+} nanophosphor. Sharp and intense X-ray diffraction peaks were observed due to formation of high crystallinity. The obtained peaks are well matched with the standard JCPDS card no. 84-0655 [19]. The average crystallite size of the Eu^{3+} doped silicate sample was estimated by using Scherer's method [20], d = kλ/βcosθ, where λ is the wavelength of X-ray (λ = 1.54 Å), β is full width at half maxima (FWHM) in radians, θ is the Bragg's angle. The average crystallite size was found to be ~ (30-40) nm. Further, crystallite size was estimated using W-H plots [21] shown in the Fig. 3, by using $\beta\cos\theta = \dfrac{0.9\lambda}{D} + 4\varepsilon\sin\theta$ where, D is the average particle size, β is the FWHM, 'θ' is the Bragg 's angle, 'λ' is the X-ray wavelength, ε is the strain. The average crystallite size estimated from Scherrer's method and W-H plots are well matched.
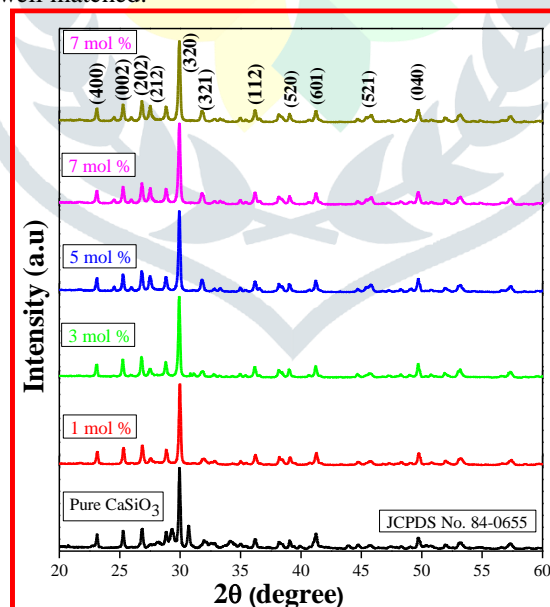

Fig.2. Powder X-ray diffraction pattern of (1-9 mol%) Eu^{3+} doped $CaSiO_3$ nanophosphor.
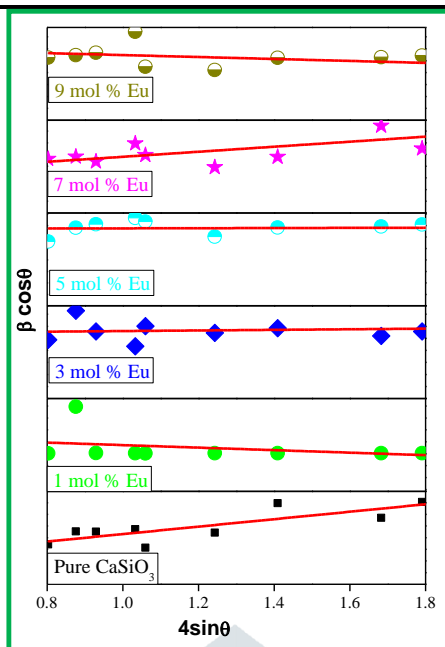
Fig.3. W-H plots of (1-9 mol%) Eu^{3+} doped $CaSiO_3$ nanophosphor.

Table.1. Estimated Average particle size of $CaSiO_3:Eu^{3+}$ (1-9 mol%) nanophosphor.

Sl. No.	mol %	Scherer's equation. in nm.	W-H Plot. in nm.	Lattice strain ϵ x10^{-3}
01	Pure	38	40	0.24
02	1	30	33	0.8
03	3	35	38	0.17
04	5	37	39	0.385
05	7	31	35	1.83
06	9	36	39	1.3

Fig. 4 (a-e) shows the FESEM images of $CaSiO_3:Eu^{3+}$(1-9 mol %) nanophosphor. As can be visualized from the Fig. 4 (a-e) the product was highly porous, fluffy and agglomerated. The porous and agglomerated morphological behavior was mainly due to the escaping of large amount of gases during combustion synthesis process. The combustion reaction depends on the formation of metal-ligand complex as a result flaming reaction takes place by discharging a large amount of toxic gases. The ligand citric acid easily influence the formation of uniform complex structure with Eu^{3+} metal ion than Ca^{2+} metal ion due to its ionic nature and variable coordination. Therefore, the porous nature of the silicate material mainly depends on the type of the metal ion used. The EDAX pattern of 7 mol % shown elements present in the prepared sample in Fig. 4 (f) and its inset of Fig. 4 (f) shows Eu^{3+} doped $CaSiO_3$ nanophosphor shows the % of elements present in the obtained material.
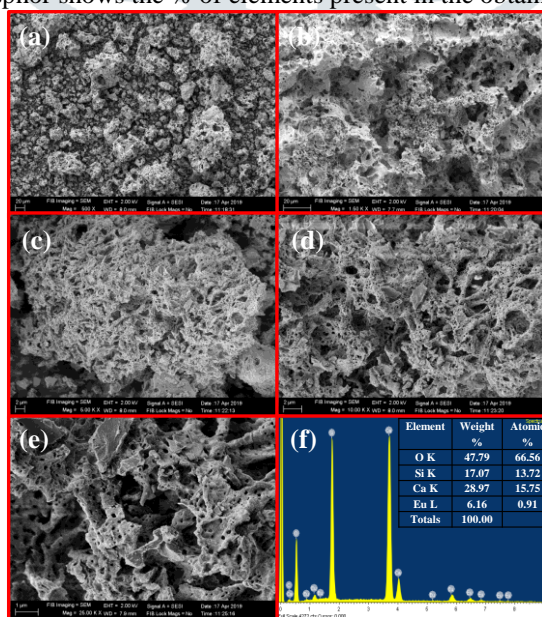

Fig.4. FESEM of (a-e) (1-9 mol %) (f) EDAX (7 mol %) images of Eu^{3+} doped $CaSiO_3$ nanophosphor.

Fourier transform infrared (FTIR) spectra of (1-9 mol %) Eu^{3+} doped $CaSiO_3$ samples synthesized via combustion method is recorded in the range 400-4000 cm^{-1} using KBr pellets is shown in Fig.5. The spectra shows the broad band at 937 cm^{-1} is due to asymmetric stretching vibration of Si–O–Si bond and stretching vibrations of terminal Si–O bonds. The peaks at 461,

555 and 691 cm^{-1} are the characteristic stretching vibrations Si–O–Si bridges [22]. The sharp peak corresponding to   691 cm^{-1} can be ascribed to Si–O bond, which exists in the form of SiO$_3^-$.
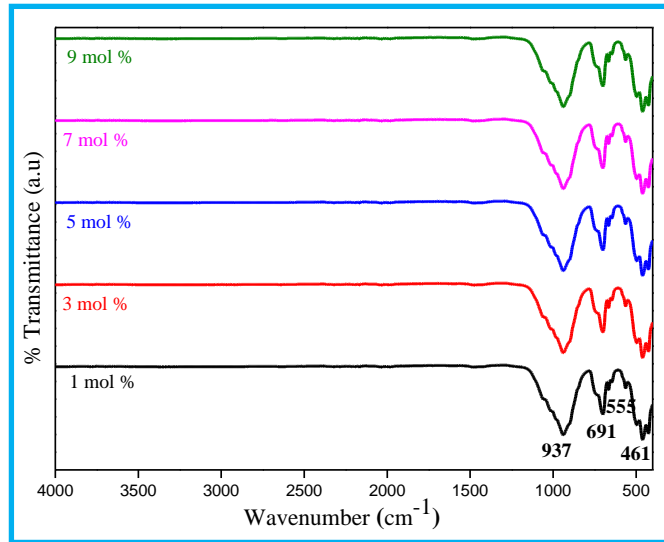

Fig.5. FTIR of (1-9 mol%) Eu^{3+} doped CaSiO$_3$ nanophosphor.

        Fig. 6 shows DRS spectra of CaSiO$_3$:Eu^{3+} (1-9 mol%) nanophosphors was shown in Fig.6 recorded at room temperature (RT). It is well established that nano scale materials have large surface to volume ratio. This results in the formation of voids on the surface as well inside the agglomerated nano particles. The surfaces of nano particles are well known to comprise of several defects such as dangling bonds, regions of disorder and absorption of impurity species that result in the absorption of nano crystals. Thus in the UV-absorption spectrum of nano crystals shows absorption bands at 434 nm are identified with the excitation of 4-fold and 3-fold co-ordinated O^{2-} anions in edges and corners (also called F$^+$, F centres.) respectively. The optical energy gap (E$_g$) of Eu^{3+} (1-9 mol%) doped CaSiO$_3$ nanophospher prepared through combustion technique was calculated using Kubelka-Munk method, DRS of the material was converted to the absorption spectra by using Kubelka – Munk function [23] and its Eg values was found to be in the rage (4.0-4.2) eV shown in the Fig. 7.
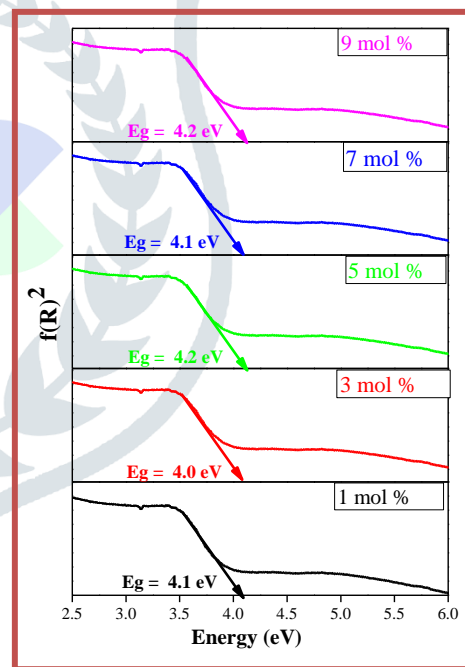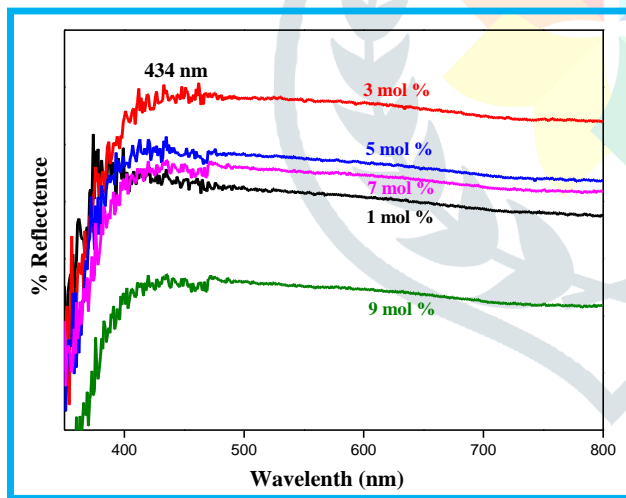

Fig.6. DRS spectra of CaSiO$_3$:Eu^{3+} (1-9 mol%) nanophosphor and **Fig.7.**Energy band gap of (1-9 mol%) Eu^{3+} doped CaSiO$_3$
        nanophosphor

        The PL emission spectra of (1-9 mol %) Eu^{3+} doped CaSiO$_3$ nanophosphor measured upon 316 nm excitation are shown in the Fig. 8. The emission bands observed are attributed to Eu^{3+} ions and are assigned to at $^5D_0 \rightarrow ^7F_0$ (566 nm), $^5D_0 \rightarrow ^7F_1$ (590 nm), $^5D_0 \rightarrow ^7F_2$ (615 nm) and $^5D_0 \rightarrow ^7F_4$ (701 nm) transitions, respectively [24-26]. The 596 nm emission corresponding to $^5D_0 \rightarrow ^7F_1$ transmission is mainly due to magnetic dipole transition which is independent of site symmetry where Eu^{3+} is positioned. The strongest emission peak at 615 nm corresponding to $^5D_0 \rightarrow ^7F_2$ is due to hypersensitive forced electric-dipole transition. As we know that Eu^{3+} occupies the centre of symmetry (spherically symmetric site) the $^5D_0 \rightarrow ^7F_2$ transition intensity is very weak for higher site symmetry as this transition intensity increases the site symmetry decreases [27]. The weaker emission peaks at 701 nm are due to the weak interaction between Eu^{3+} and O^{2-} ions present in CaSiO$_3$:Eu^{3+} nanophosphor.

        From Fig.8. it is observed that the emission intensity increased with increase in Eu^{3+} concentration upto 7 mol% and there after it decreased with further increase in concentration [28], observed the similar behavior in CaSiO$_3$:Eu^{3+} nanophosphor prepared by solution combustion technique where the PL intensity was attributed to the ionic radius of Eu^{3+} and Ca^{2+} ions. This showed that ionic radius and charge state of the impurity ion acts as a major contributors in the emission spectra. Initially, the PL intensity increases with increase in Eu^{3+} concentration because the ionic radius of Eu^{3+} (1.13 Å) was slightly bigger than Ca^{2+} (1.14 Å), therefore a small percentage of impurity ions can only accommodate in the CaSiO$_3$ host matrix. Further, with increase in the Eu^{3+} concentration the charge imbalance may occur as a consequence, trapping centres are created. This trapping centres results in cross relaxation due to which concentration quenching takes place.
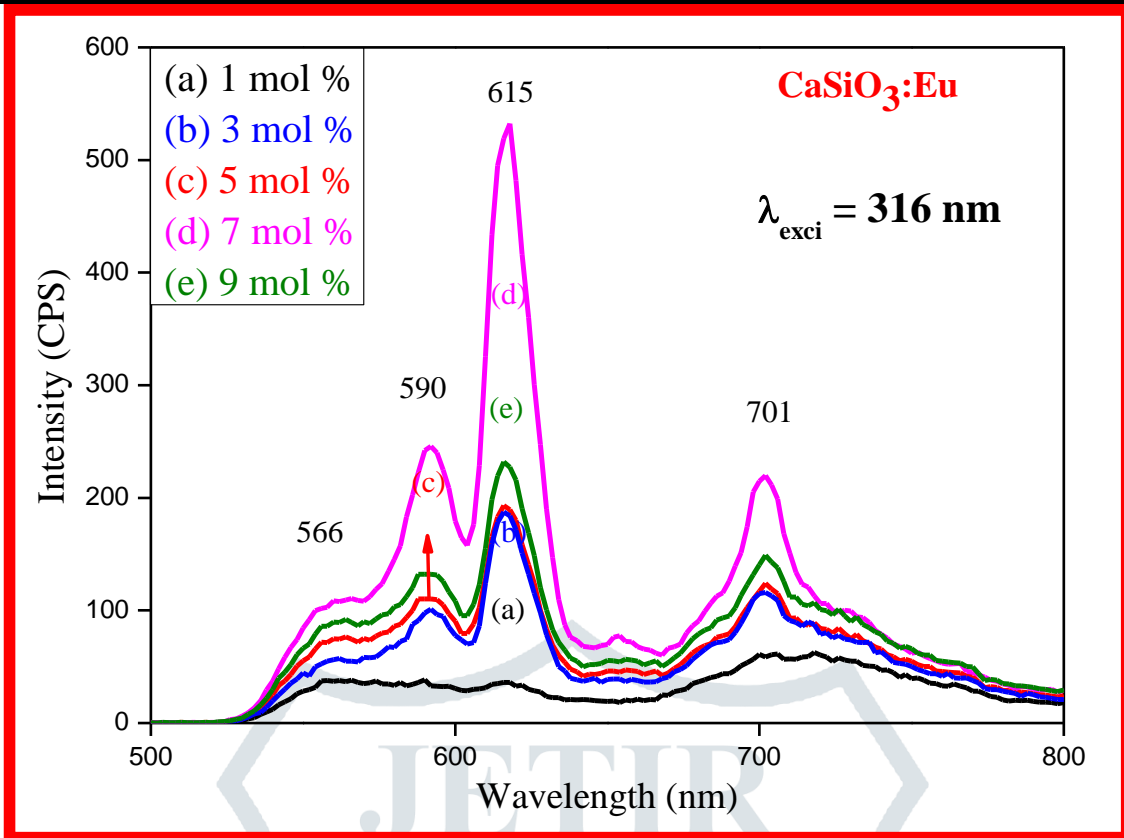
Fig. 8. PL emission spectra of $CaSiO_3$:Eu^{3+} (1-9 mol%) nanophosphor.

  The luminous color was depicted by studying color co-ordinates and color ratios of the phosphor. The values of chromaticity co-ordinates of the $CaSiO_3$:Eu^{3+} (1-9 mol %) phosphor have been estimated from 1931 CIE system and was shown in Fig. 9 (a). It was observed that the CIE co-ordinates of (1-9 mol%) Eu^{3+} activated $CaSiO_3$:Eu^{3+} phosphor was measured and x and y values are tabulated in the inset Fig.9. Which was very close to the NTSC standard values and it was supported by CCT of (1-9 mol %) Eu^{3+} doped $CaSiO_3$ nanophosphor shown in the Fig. 9(b) also, u′, v′ and CCT values given the table of inset Fig. 9 (b) [29]. Their corresponding location has been marked in Fig. 9(b). with star mark in red region. Hence of (1-9 mol %) Eu^{3+} doped $CaSiO_3$ nanophosphor is suitable material for preparation of red component of WLEDs and display applications.
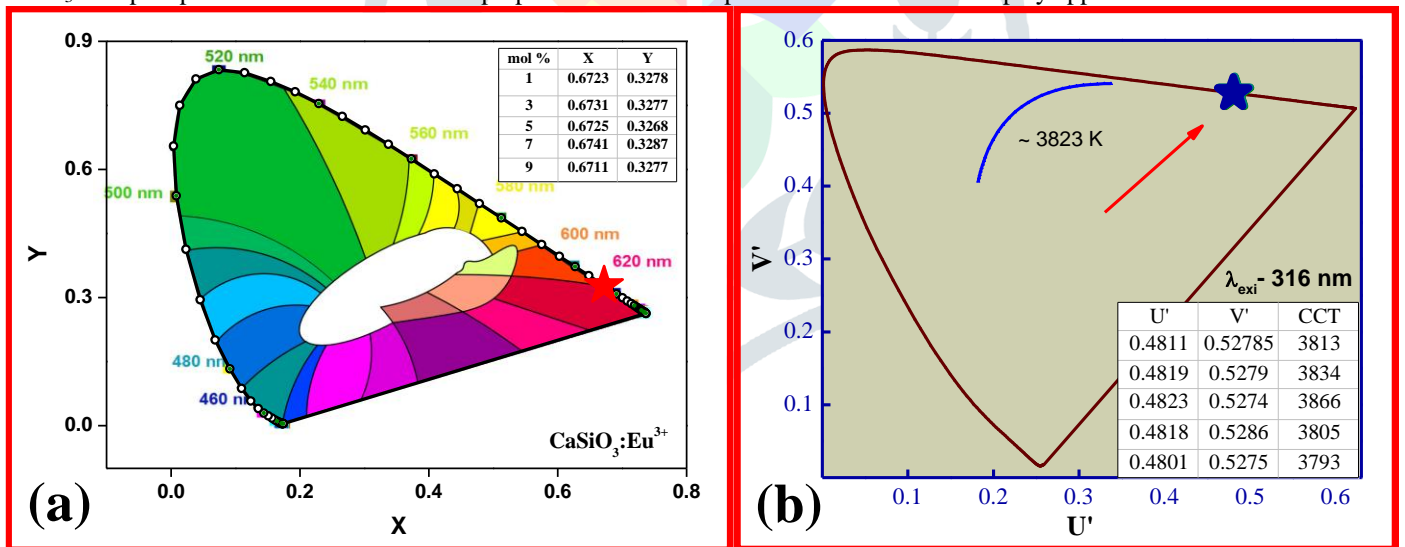

Fig. 9 (a). CIE (Inset: table of x and y values) **(b)** CCT (Inset: table of u′, v′ and CCT values)of $CaSiO_3$:Eu^{3+} (1-9 mol%) nanophosphor

VI. Conclusions

  $CaSiO_3$:Eu^{3+} (1-9 mol%) nanophosphors were succefully prepared by solution combustion technique and was subjected to structural characterization and luminescent studies. PXRD patterns showed that the obtained nanopowders were highly crystalline, nano in size about (30-40) nm and shows monoclinic phase. The porous and agglomerated morphology seen in $CaSiO_3$:Eu^{3+} (1-9 mol %) nanophosphor was due to the escaping of gases during synthesis process. FTIR of prepared samples shows the purity of the compound. Energy gap of in the range of (4.00-4.2) eV prepared sample shows insulating nature of the sample taking by UV visible spectra. The PL studies in $CaSiO_3$:Eu^{3+} (1-9 mol %) nanophosphor reveled the Eu^{3+} peaks at 566, 590, 615 and 701 nm excited at 316 nm corresponding to $^5D_0 \rightarrow {}^7F_0$, $^5D_0 \rightarrow {}^7F_1$, $^5D_0 \rightarrow {}^7F_2$, and $^5D_0 \rightarrow {}^7F_4$ transitions respectively. The highest PL intensity was observed in 7 mol % Eu^{3+} doped $CdSiO_3$ nanophosphor. Hence, the sample can be effectively excited by radiations of wavelength in the 316 nm and emitted radiations of wavelength 615 nm with more intensity. So it confirms from CIE and CCT plots. Hence 7 mol % Eu^{3+} doped $CaSiO_3$ nanophosphor can be used as a red component of white LEDs and also used in preparation of display applications.

REFERENCES

[1]. V. Kumar, R. Kumar, N. Singh, S.P. Lochab, J. Phys. D: Appl. Phys. 39 (2006) 5137-5142.

[2]. B.F. Lei, B. Li, X.J. Wang, W.L. Li, J. Lumin. 118 (2006) 173–178.

[3]. L. Zhang, G.Y. Hong, X.L. Sun, Chin. Chem. Lett. 10 (1999) 799–802.

[4]. B. Lei, Y. Liu, Z. Ye, C. Shi, J. Lumin. 109 (2004) 215–219.

[5]. M. Wanga, X. Zhang, Z. Hao, X. Ren, Y. Luo, X. Wang, J. Zhang, Opt. Mat. 32 (2010) 1042–1045.

[6]. L. Zhang, X. Zhou, H. Zeng, H. Chen, X. Dong, Mat. Letts. 62 (2008) 2539–2541.

[7]. C.Bull, G.F.J.Garlick, J. Electrochem. Soc. 93(1951) 371-375.

[8]. K.J.Yong, L.Y.Liang, Chin. Phys. Lett., 23 (2006) 204-206.

[9]. B.F. Lei, Y.L. Liu, J. Liu, Z.R. Ye, C.S. Shi, J. Solid State Chem. 177 (2004) 1333-1337.

[10]. L. C.V. Rodrigues, H. F. Brito, J. Holsa, R. Stefani, M. C.F.C. Felinto, M. Lastusaari, T. Laamanen, L. A.O. Nunes, J. Phys. Chem. C, 116 (2012) 11232−11240.

[11]. R. Krsmanovic, Z. Antic, I. Zekovic, M. D. Dramicanin, J. Alloys Compds, 480 (2009) 494–498.

[12]. H. Chang, H. D. Park, K. S. Sohn, J. D. Lee, J.l of the Korean Phys. Soc., 34 (1999) 545-548.

[13]. L.Lin, C. Shi, Z. Wang, W. Zhang, M. Yin, J. of Alloys and Compds., 466 (2008) 546–550.

[14]. L. Yang, M. Fang, L. Du, Z. Zhang, L. Ren, X. Yu, Mater. Res. Bull., 43 (2008) 2538–2543.

[15]. C. A. Barboza, J. M. Henriques, E. L. Albuquerque, E. W. S. Caetano, V. N. Freire, L. A. O. da Costa, Chem. Phys. Lett. 480 (2009) 273-277.

[16]. B. F.Lei, Y. L. Liu, Z. R. Ye, C. S. Shi, Chin. Chem. Letts., 15 (2004) 335-338.

[17]. K.C. Patil, S.T. Aruna, S. Ekambaram, Curr. Opin. Solid State Mater. Sci. 457 (1997) 158–165.

[18]. K.C. Patil, M.S. Hegde, Tanu Rattan, S.T. Aruna, Chemistry of Nanocrystalline Oxide Materials, Combustion Synthesis, Properties and Applications, World Scientific Publishing Co. Pvt. Ltd., Singapore, 2008.

[19]. Lei Zhou, Bing Yan, Sol–gel synthesis and photoluminescence of $CaSiO_3$:Eu^{3+} nanophosphors using novel silicate sources, Journal of Physics and Chemistry of Solids, 69-11 (2008) 2877-2882..

[20]. P. Klug, L.E. Alexander, In: X-ray Diffraction Procedure,Wiley, New York, 1954.

[21]. G.K. Williamson, W.H. Hall, Acta Metall. 1 (1953) 22–31.

[22]. R.P. S. Chakradar, B.M. Nagabhushna, G.T. Chandrappa, K.P. Ramesh, J.L. Rao, Mater. Chem. Phys. 95 (2006) 169–175.

[23] A. Escobedo Morales, E. Sanchez Mora, U. Pal, Use of diffuse reflectance spectroscopy for optical characterization of un-supported nanostructures, Rev. Mexic. De Fisica S 53 (2007)   18-22.

[24]. J.Yang, Z. Quan, D. Kong, X. Liu, J. Lin, Cryst. Growth and Des., 7 (2007) 730-735.

[25]. Q. Yanmin, Z. Xinbo, Y. Xiao, C.Yan, G.Hai, J. Rare Earths, 27 (2009) 323-326.

[26]. Lei Zhou, Bing Yan, J. Phys. Chem., Solids 69 (2008) 2877–2882

[27]. D.V. Sunitha, H.Nagabhushana, F. Singh, B.M.Nagabhushana, S.C. Sharma, R.P.S.Chakradhar, J. Lumin., 132 (2012) 2065–2071.

[28]. H. Nagabhushana, B.M. Nagabhushana, M. Madesh Kumar, C. Rayappa, K.V.R. Murthy, C. Shivakumara, R.P.S. Chakradhar, Spectrochim. Acta Part A 78 (2011) 64–69.

[29]. B. M. Manohara, H. Nagabhushana, K. Thyagarajan, B. D. Prasad, S.C. Prashantha, S. C. Sharma and B. M. Nagabhushana, "Spectroscopic and luminescence studiesof Cr^{3+} doped cadmium silicate nano-phosphor," J. Lumin., 161 (2015) 247–256.